Protein Science (1998), 7:1071–1082. Cambridge University Press. Printed in the USA.

Refolding rate of stability-enhanced cytochrome *c* is independent of thermodynamic driving force

WILLIAM A. McGEE AND BARRY T. NALL

Department of Biochemistry, University of Texas Health Science Center, San Antonio, Texas 78284-7760

(RECEIVED October 20, 1997; ACCEPTED January 22, 1998)

Abstract

N52I iso-2 cytochrome *c* is a variant of yeast iso-2 cytochrome *c* in which asparagine substitutes for isoleucine 52 in an alpha helical segment composed of residues 49–56. The N52I substitution results in a significant increase in both stability and cooperativity of equilibrium unfolding, and acts as a "global suppressor" of destabilizing mutations. The equilibrium *m*-value for denaturant-induced unfolding of N52I iso-2 increases by 30%, a surprisingly large amount for a single residue substitution. The folding/unfolding kinetics for N52I iso-2 have been measured by stopped-flow mixing and by manual mixing, and are compared to the kinetics of folding/unfolding of wild-type protein, iso-2 cytochrome *c*. The results show that the observable folding rate and the guanidine hydrochloride dependence of the folding rate are the same for iso-2 and N52I iso-2, despite the greater thermodynamic stability of N52I iso-2. Thus, there is no linear free-energy relationship between mutation-induced changes in stability and observable refolding rates. However, for N52I iso-2 the unfolding rate is slower and the guanidine hydrochloride dependence of the unfolding rate is smaller than for iso-2. The differences in the denaturant dependence of the unfolding rates suggest that the N52I substitution decreases the change in the solvent accessible hydrophobic surface between the native state and the transition state. Two aspects of the results are inconsistent with a two-state folding/unfolding mechanism and imply the presence of folding intermediates: (1) observable refolding rate constants calculated from the two-state mechanism by combining equilibrium data and unfolding rate measurements deviate from the observed refolding rate constants; (2) kinetically unresolved signal changes ("burst phase") are observed for both N52I iso-2 and iso-2 refolding. The "burst phase" amplitude is larger for N52I iso-2 than for iso-2, suggesting that the intermediates formed during the "burst phase" are stabilized by the N52I substitution.

Keywords: free energy; global suppressors; iso-2 cytochrome *c*; protein folding; yeast

The stability enhancing properties of the asparagine to isoleucine (N52I) substitution at position 52 in cytochrome *c* are well known from extensive thermodynamic and X-ray crystallographic studies of N52I iso-1 cytochrome *c* (Das et al., 1989; Hickey et al., 1991; Berghuis et al., 1994; Komar-Panicucci et al., 1994) and N52I iso-2 cytochrome *c* (Fig. 1) (McGee et al., 1996). For example, scanning calorimetry measurements of thermal unfolding of N52I iso-2 show that the N52I substitution increases the stability of both the oxidized and reduced forms by 2–3 kcal/mol (McGee et al., 1996). The N52I substitution is also known to act as a "global suppressor" mutation (Shortle & Lin, 1985) by reverting other nonfunctional (second site) mutations to yield functional cytochrome *c* (Berroteran & Hampsey, 1991). The X-ray crystallographic structures of N52I iso-1 (Berghuis et al., 1994) and N52I iso-2 (McGee et al., 1996) show a substantial rearrangement in the hydrogen bonding of residues near the heme that results in the loss of a conserved water molecule, denoted Wat106 in iso-2 (Murphy et al., 1992) (Fig. 2A,B). The N52I substitution, while compatible with function, alters the electrochemical properties of the protein by reducing E_m, the midpoint potential (Gao et al., 1992; Berghuis et al., 1994; McGee et al., 1996). For example at 25 °C, E_m = 288 mV for iso-2 and E_m = 243 mV for N52I iso-2 (McGee et al., 1996).

Energetic relationships between folding intermediates, transition states, and the native state may provide insight into the structural determinants of protein folding pathways. One test for structural and energetic similarity between the folding transition state and the native conformation is the relationship between equilibrium free energies and activation free energies of folding (Matouschek & Fersht, 1993; Matthews & Fersht, 1995). Tests for a relationship between stability and folding rates for cytochromes *c* have compared the kinetics of folding of yeast iso cytochromes *c* (Nall & Landers, 1981; Mines et al., 1996) to the folding kinetics of the more stable horse cytochrome *c* (Ikai et al., 1973; Tsong, 1976).

Reprint requests to: Barry T. Nall, Department of Biochemistry, University of Texas Health Science Center, 7703 Floyd Curl Drive, San Antonio, Texas 78284-7760; e-mail: nall@bioc01.uthscsa.edu.

Fig. 1. Ribbon diagram of yeast iso-2 cytochrome *c*. The heme (red) is linked through thioether bonds to Cys14 and Cys17 (yellow) to the polypeptide. The side-chain heme ligands, His18 and Met80 (cyan), form coordinate bonds to the heme. Asn52 (green) is the position of the substitution to Ile. Trp59 (blue) is the fluorescence probe used to monitor folding. Coordinates are from the X-ray structure of iso-2 (Murphy et al., 1992; Murphy, 1993).

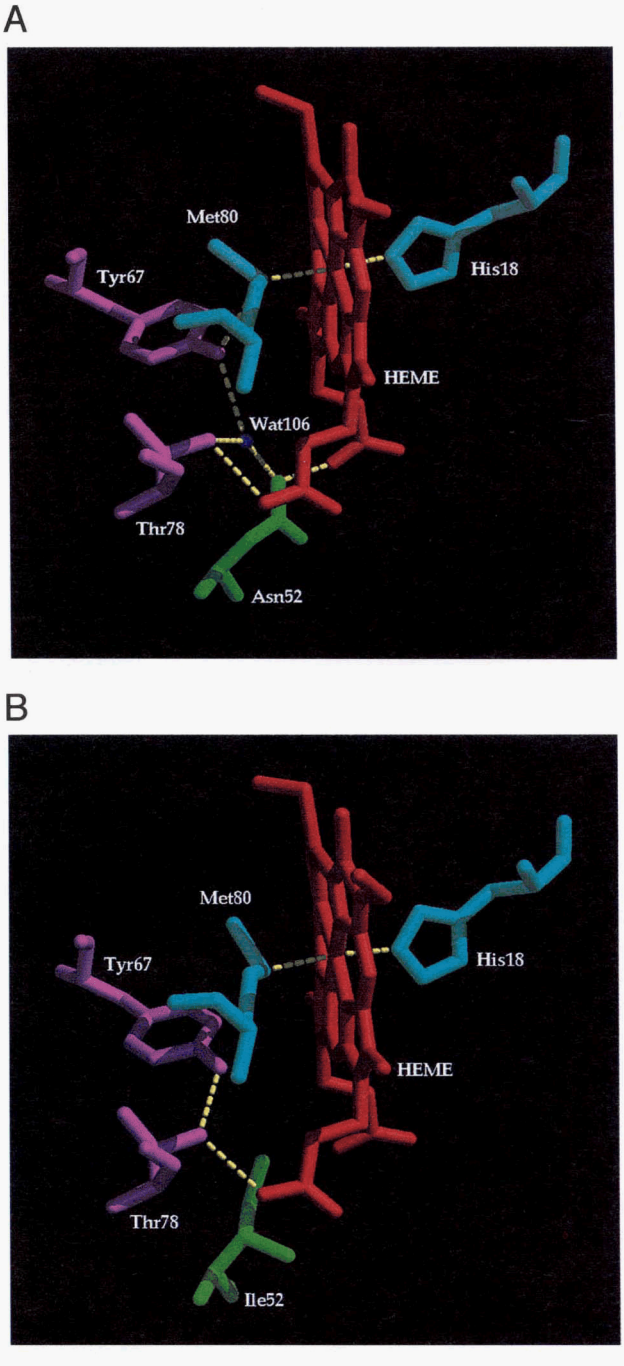

Fig. 2. Diagram of active site region of (**A**) iso-2 and (**B**) N52I iso-2 showing the structural differences between iso-2 and the stability-enhanced variant, N52I iso-2. The N52I substitution leads to a change in hydrogen bonding and loss of conserved Wat106. The hydrogen bond between the Tyr67 O–H and a sulfur lone pair of Met80 is broken. Other changes include hydrogen bonds involving Thr78 and the heme propionates. Coordinates are from the X-ray structures of iso-2 (Murphy et al., 1992; Murphy, 1993) and N52I iso-2 (McGee et al., 1996).

Horse and yeast cytochromes *c* have large differences in the standard free energy of unfolding: $\Delta G^{\circ}_{U} = 4.2$–$4.9$ kcal mol^{-1} for iso-2 (Veeraraghavan et al., 1995; McGee et al., 1996); $\Delta G^{\circ}_{U} = 7.3$ kcal mol^{-1} for horse cytochrome *c* (Knapp & Pace, 1974). Despite the large stability difference, the horse and yeast homologues share essentially the same backbone fold (Louie & Brayer, 1990; Murphy et al., 1992). A relationship between thermodynamic stability and folding rates, if present, should be readily detected by comparing these distantly related members of the mitochondrial cytochrome *c* family. There are two ways of testing the linear free energy hypothesis: refolding rates for cytochrome *c* homologues can be compared (1) at the same thermodynamic stability by adjusting the final denaturant concentration, or (2) at different thermodynamic stabilities under the same refolding conditions, for example, same denaturant concentration, temperature, pH. The observation that folding rates for horse and yeast iso-2 cytochromes *c* are similar when compared at the same thermodynamic stability (Nall & Landers, 1981) is in accord with the linear free-energy hypothesis. Refolding compared at different thermodynamic stabilities is also in accord with a linear relationship between equilibrium free energies and activation free energies for folding: folding of the more stable horse cytochrome *c* is substantially faster than folding of less stable yeast iso-1 (Mines et al., 1996). Results reported here for the kinetics of folding of N52I iso-2 provide an exception to the linear free energy "rule": stability is increased, but the refolding rate is unchanged.

Quantitative predictions of refolding rates from a two-state analysis combining equilibrium unfolding data and kinetic unfolding rate measurements provide an important test for the presence of folding intermediates (Matouschek et al., 1990). Equilibrium unfolding experiments are carried out to determine the denaturant dependence of the unfolding equilibrium constant, K_u. Similarly, unfolding kinetic experiments measure the denaturant dependence of the unfolding rate constant, k_u. The unfolding rate measurements are carried out above the transition midpoint where the

formation of intermediates is unlikely and a two state kinetic analysis is feasible. By combining the equilibrium and kinetic measurements, the dependence of the refolding rate, k_f, on denaturant concentration is calculated from the two-state model: $k_f = k_u/K_u$. Evidence of intermediates is obtained when the calculated values of k_f exceed those measured directly in refolding kinetic experiments. An important consequence of this approach is that an estimate of the stability of intermediates is also obtained. Application of this test to N52I iso-2 and iso-2 shows that there are significant deviations from the two-state model for N52I iso-2 folding, indicating that the N52I substitution stabilizes folding intermediates.

Other evidence for cytochrome *c* folding intermediates is the presence of a kinetically unresolved "burst phase" (Elove et al., 1992), which is defined as the fraction (or percent) of the equilibrium signal change that occurs at a rate too fast (<2–4 ms) to be detected by stopped-flow refolding. For horse cytochrome *c* the "burst phase" involves the rapid formation of a compact state early in folding (Colon et al., 1996), which may be a nonspecific response of the unfolded protein to low denaturant concentration (Sosnick et al., 1997). A "burst phase" has also been reported for the kinetics of folding of iso-2 (Nall, 1983). Typically, the "burst phase" amplitude is strongly dependent on denaturant concentration present in the final folding conditions. For refolding at 0.25 M Gdn·HCl, 20 °C, over half of the signal change occurs in the "burst phase" for N52I iso-2 compared to about 15% for iso-2, indicating that the N52I substitution enhances the population of "burst phase" intermediates.

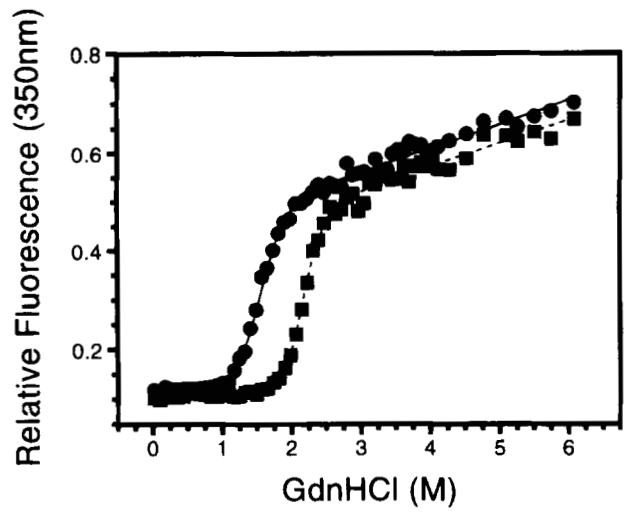

Fig. 3. Guanidine hydrochloride induced equilibrium unfolding of iso-2 (circles) and N52I iso-2 (squares) at 20 °C, 0.1 M sodium phosphate, pH 6.0. Fluorescence at 350 nm (excitation 285 nm) relative to the fluorescence of an equal molar concentration of N-acetyltryptophanamide is measured as a function of guanidine hydrochloride concentration. The protein concentrations were 4 μM. The curves were analyzed using the method described by Santoro and Bolen (1988) with the program ENZFITTER (Leatherbarrow, 1987). The best fits to the nonlinear least-squares analysis are shown by the lines through the data. The parameters are listed in Table 1.

Results

Equilibrium unfolding

Figure 3 shows the Gdn·HCl-induced equilibrium unfolding curves of iso-2 and N52I iso-2 monitored by fluorescence emission at 350 nm. A shift in C_m, the transition midpoint, to higher Gdn·HCl is evident for N52I iso-2 (filled squares). Thermodynamic parameters are obtained by analyzing the data using the linear extrapolation model according to Santoro and Bolen (Santoro & Bolen, 1988). As summarized in Table 1, the N52I substitution changes all three of the parameters describing the unfolding transition: C_m is increased by 0.7 M Gdn·HCl; ΔG°_U by 3.9 kcal mol^{-1}; and the *m*-value by almost 30%.

Folding/unfolding kinetics

Figure 4 compares kinetic traces for fast phase (τ_2) refolding of iso-2 (Fig. 4A) and N52I iso-2 (Fig. 4B) at the same final Gdn·HCl concentration. The refolding conditions strongly favor formation of native structure for both proteins, although the thermodynamic driving force ($-\Delta G_U$) is substantially greater for N52I iso-2. For example, the equilibrium parameters in Table 1 can be used to calculate the equilibrium folding free energy at the final refolding conditions for both proteins: $-\Delta G_U$(0.6 M) = −2.8 ± 0.3 kcal mol^{-1} for iso-2; $-\Delta G_U$(0.6 M) = −6.2 ± 0.5 kcal mol^{-1} for N52I iso-2. Figure 4 shows that the apparent rate for fast phase (τ_2) refolding ($k_{obs} = 1/\tau_2$) is the same, despite the differences in the equilibrium unfolding free energy. This result is in direct conflict with expectations of a linear free energy "rule" for refolding, which requires the activation free energy for folding to be proportional to the equilibrium unfolding free energy.

Figure 5 compares kinetic traces for fast phase (τ_2) unfolding of iso-2 (Fig. 5A) and N52I iso-2 (Fig. 5B) at the same final Gdn·HCl concentration. Unfolding is complete for both proteins in the final unfolding conditions, although for N52I iso-2 the final unfolding equilibrium is very close to the upper edge of the unfolding transition zone (Fig. 3). The equilibrium parameters in Table 1 can be used to calculate the thermodynamic driving forces favoring unfolding for the two proteins. The calculation gives equilibrium unfolding free energies in the final unfolding conditions of ΔG_U(2.8 M) = −3.8 ± 0.3 kcal mol^{-1} for iso-2; and ΔG_U(2.8 M) = −2.4 ± 0.2 kcal mol^{-1} for N52I iso-2. As shown in Figure 5, the apparent rate for fast phase (τ_2) unfolding is much slower for unfolding of N52I iso-2 than for iso-2. Thus, the free energy difference caused by the N52I substitution shows up largely in the slower unfolding rate, and not at all in refolding.

The Gdn·HCl dependence of the amplitudes and rates for fluorescence-detected refolding and unfolding is given in Figures 6 (iso-2) and 7 (N52I iso-2). Similar data for the absorbance-detected folding/unfolding kinetics are presented in Figure S1 (supplementary materials) for iso-2 and Figure S2 (supplementary materials) for N52I iso-2. The data presented in Figures 6 and 7, and S1 and S2 (supplementary materials) show that the fast phase (τ_2) refolding for iso-2 and N52I iso-2 is essentially the same for both proteins whether probed by absorbance or fluorescence. For unfolding kinetic experiments the results are also essentially the same whether folding is monitored by absorbance or fluorescence. However, throughout the entire unfolding branch of the τ_2 kinetic phase, unfolding of N52I iso-2 is much slower than unfolding of iso-2. The iso-2 kinetic data presented in Figures 6 and S1 (supplementary material) are in good agreement with previous results (Nall & Landers, 1981; Nall, 1983; Osterhout & Nall, 1985; Nall et al., 1988). The rate of slow phase (τ_{1b}) fluorescence-detected

Table 1. *Equilibrium unfolding for iso-2 and N52I iso-2*[a]

Protein	ΔG_U° (kcal mol^{-1})	K_U°	m (kcal mol^{-1} M^{-1})	C_m (M)
Iso-2	4.6 ± 0.3	(3.6 ± 0.1) × 10^{-4}	3.0 ± 0.2	1.5 ± 0.2
N52I iso-2	8.5 ± 0.5	(5.0 ± 0.1) × 10^{-7}	3.9 ± 0.2	2.2 ± 0.2

[a]The fluorescence equilibrium unfolding parameters for iso-2 and N52I iso-2, at 20 °C, 0.1 M sodium phosphate, pH 6.0, and protein concentrations of 4.1 μM. The values for ΔG_U°, C_m, and m were obtained using the linear extrapolation model as described by Santoro and Bolen (1988). K_U° is the equilibrium constant in 0.1 M Na phosphate, pH 6, 20 °C determined from the value for ΔG_U° as follows: $K_U^\circ = \exp(-\Delta G_U^\circ/RT)$. Errors are estimated from the statistics of nonlinear least-squares fits of the data (see Fig. 3) using the program ENZFITTER (Leatherbarrow, 1987).

folding is the same for iso-2 and N52I iso-2 (compare Figs. 6B and 7B). Moreover, the rate of slow phase (τ_{1a}) absorbance-detected folding is the same for iso-2 and N52I iso-2 (compare Figs. S1B and S2B; supplementary materials). However, as has been previously reported (Nall, 1983), slow folding monitored by fluorescence (τ_{1b}) is somewhat faster than slow folding monitored by absorbance (τ_{1a}). Thus, the small difference in the rates for absorbance-detected and fluorescence-detected slow folding is re-

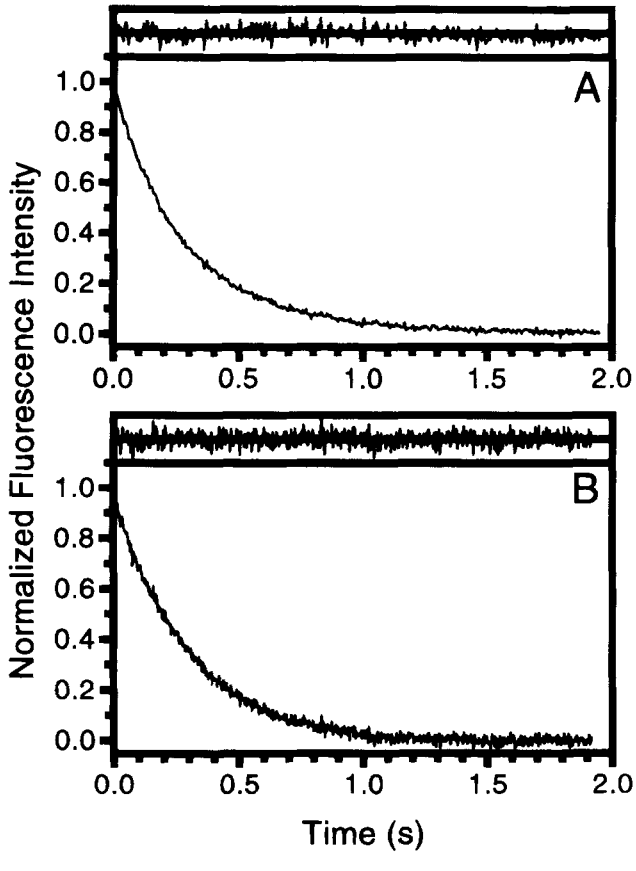

Fig. 4. Kinetic traces showing the similarity in rates for fluorescence-detected fast phase (τ_2) refolding for (**A**) iso-2 and (**B**) N52I iso-2. The initial conditions are: 200 μM iso-2 or 275 μM N52I iso-2 unfolded in 4.5 M Gdn·HCl, 0.1 M sodium phosphate, pH 6, 20 °C. The final refolding conditions are: 10 μM iso-2 or 9.2 μM N52I iso-2, 0.6 M Gdn·HCl, 0.1 M sodium phosphate, pH 6.0, 20 °C. The data points are fit to a function of the form: $S(t) = A_2\exp(-t/\tau_2)$ where A_2 and τ_2 are the amplitude and time constant for the fast folding phase. The fit to $S(t)$ gives the following parameters: (**A**) A_2 = 1.94 V, τ_2 = 279 ms for iso-2; and (**B**) A_2 = 1.84 V, τ_2 = 287 ms for N52I iso-2. The narrow panels at the top of each trace give residuals of the fits.

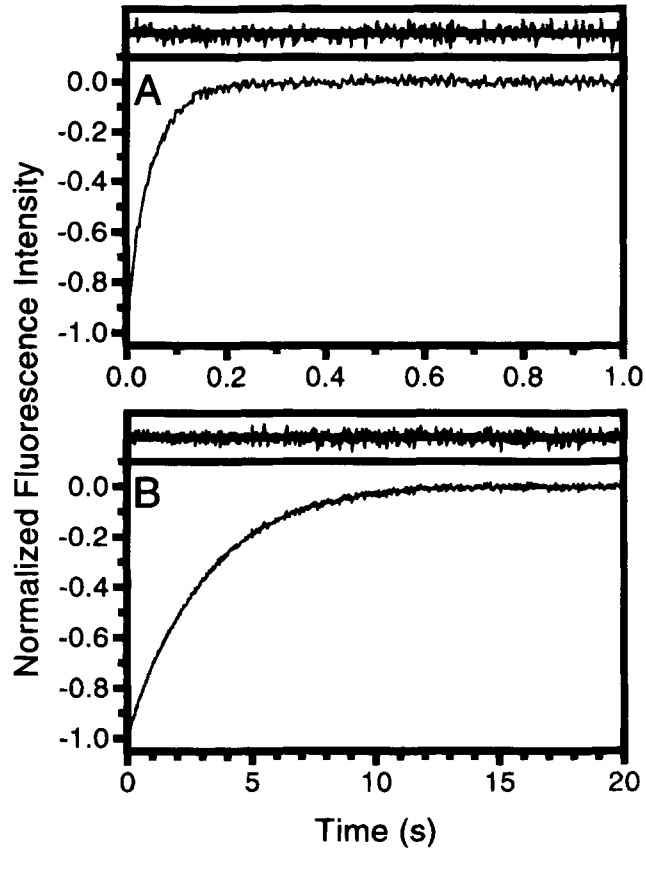

Fig. 5. Kinetic traces showing that fluorescence-detected fast phase (τ_2) unfolding is faster for (**A**) iso-2 than for (**B**) N52I iso-2. The initial conditions are: 200 μM iso-2 or 166 μM N52I iso-2 in 0.4 M Gdn·HCl, 0.1 M sodium phosphate, pH 6, 20 °C. The final unfolding conditions are: 10 μM iso-2 or 11 μM N52I iso-2, 2.8 M Gdn·HCl, 0.1 M sodium phosphate, pH 6, 20 °C. The data points are fit to a function of the form: $S(t) = A_2\exp(-t/\tau_2)$ where A_2 and τ_2 are the amplitude and time constant for the fast unfolding phase. The fit to $S(t)$ gives the following parameters: (**A**) A_2 = −0.95 V, τ_2 = 48 ms, for iso-2; and (**B**) A_2 = −1.32 V, τ_2 = 3,215 ms for N52I iso-2. The narrow panels at the top of each trace give residuals of the fits.

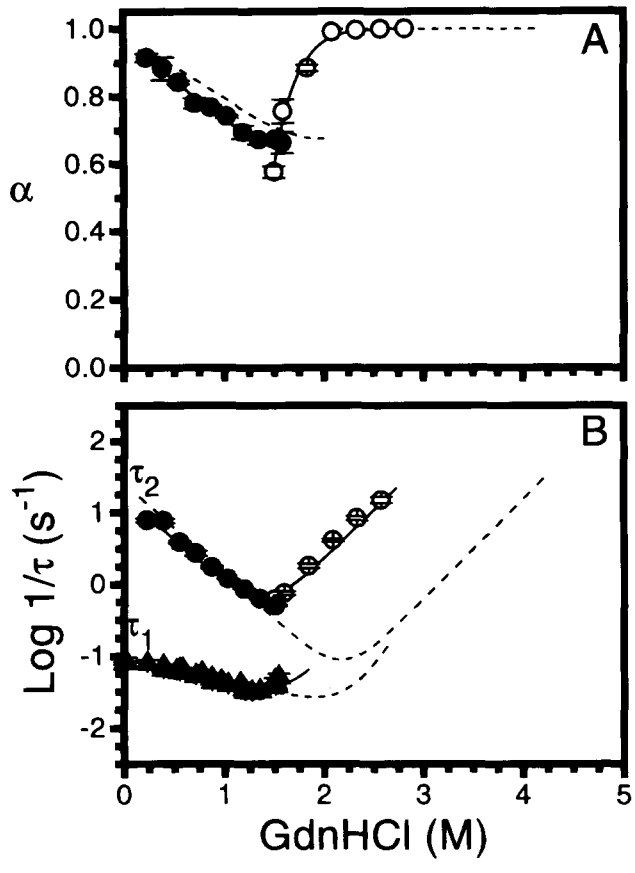

Fig. 6. The guanidine hydrochloride dependence of (**A**) relative amplitude (α) for the fast phase, and (**B**) of $\log(1/\tau)$, for the fast (τ_2) and slow (τ_1) phases in fluorescence-detected folding and unfolding for iso-2 cytochrome *c*. The filled symbols are for refolding measurements, while the open symbols are for unfolding experiments. The slow phase (τ_1) was measured by both manual mixing and stopped-flow mixing. For refolding the initial conditions were 20 °C, in 0.1 M sodium phosphate, pH 6.0 and 4.5 M Gdn·HCl. For unfolding the initial conditions were 20 °C, in 0.1 M sodium phosphate, pH 6.0 and 0.4 M Gdn·HCl. Initial protein concentrations were 200 μM for both refolding and unfolding experiments. Final conditions were 0.1 M sodium phosphate, 20 °C, at the indicated Gdn·HCl concentration. The solid line through the fast phase (τ_2) data shows the theoretical fit to a two-state kinetic model, while the dashed line shows the fit to a two-state kinetic model for the N52I iso-2 data (Fig. 7) for comparison. The theoretical curves were obtained by fitting the data to the following equation: $\log k_{obs} = \log(k_F + k_U)$; where $\log k_U = \log k_U^\circ + [m_U^\ddagger/(2.303RT)][\text{Gdn·HCl}]$, and $\log k_F = \log k_F^\circ - [m_F^\ddagger/(2.303RT)][\text{Gdn·HCl}]$. The parameters are: $k_{obs} = (1/\tau)$ is the apparent rate constant; k_F and k_U are the microscopic rate constants for folding and unfolding, respectively; k_F° and k_U° are the folding and unfolding rate constants at zero molar Gdn·HCl; $m_F^\ddagger$ and $m_U^\ddagger$ are the guanidine hydrochloride dependence of the activation free energy for folding and unfolding, respectively. Lines through the slow phase (τ_1) data and the relative amplitudes have no theoretical significance.

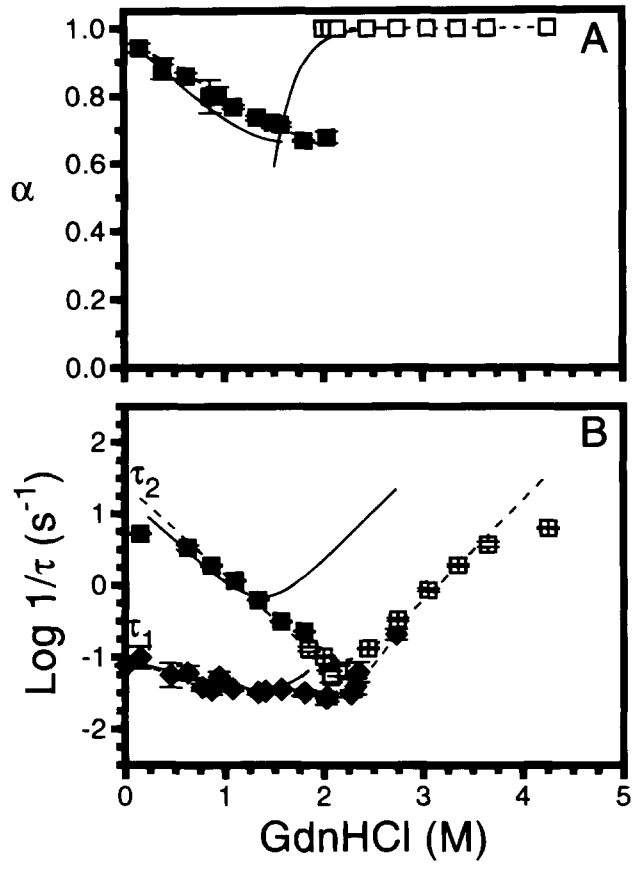

Fig. 7. The guanidine hydrochloride dependence of (**A**) the relative amplitude (α) for the fast phase, and (**B**) $\log(1/\tau)$ for the fast (τ_2) and slow (τ_1) phases in fluorescence-detected folding and unfolding for N52I iso-2 cytochrome *c*. The filled symbols are for refolding measurements, while the open symbols are for unfolding experiments. For refolding the initial conditions were 20 °C, in 0.1 M sodium phosphate, pH 6.0 and 4.5 M Gdn·HCl. For unfolding the initial conditions were 20 °C, in 0.1 M sodium phosphate, pH 6.0 and 0.4 M Gdn·HCl. Initial protein concentrations were 275 μM (refolding) and 166 μM (unfolding). Mixing ratios of 1:29 and 1:14 gave final protein concentrations for stopped-flow mixing of 9 μM (refolding) and 10 μM (unfolding). The initial protein concentrations for hand-mixing experiments were 800 μM. A mixing ratio of 1:199 gave a final protein concentration of 4 μM. Final conditions were 0.1 M sodium phosphate, pH 6, 20 °C, and the indicated Gdn·HCl concentration. The dashed line through the fast phase (τ_2) data shows the theoretical fit to a two-state kinetic model, while the solid line shows the fit to a two-state kinetic model for the iso-2 data (Fig. 6) for comparison. The theoretical curves were obtained as described in Figure 6. The lines through the slow phase (τ_1) data and the relative amplitudes (α) have no theoretical significance.

tained in the presence of the N52I substitution. Slow phase rates measured by stop-flow mixing and hand mixing experiments were in excellent agreement indicating the absence of stopped-flow artifacts arising from wide spectral band widths or baseline stability.

Two-state analysis of kinetic data

The fit of the kinetic data to a two-state mechanism was assessed using standard methods (Matouschek et al., 1990; Schindler et al., 1995). The results of these calculations can be seen in Figure 8A and B and Table 2. The observed fast phase (τ_2) unfolding rates were fit to a straight line according to the equation:

$$\log k_U = \log k_U^\circ + [m_U^\ddagger/(2.303RT)][\text{Gdn·HCl}] \quad (1)$$

were k_U is obtained from the experimental data ($k_{obs} = 1/\tau_2 \approx k_U$). k_U° is the (extrapolated) value of the unfolding rate constant in the absence of Gdn·HCl, and $m_U^\ddagger$ is the denaturant dependence of the activation free energy for unfolding ($m_U^\ddagger = d(\Delta G_U^\ddagger)/d[\text{Gdn·HCl}]$).

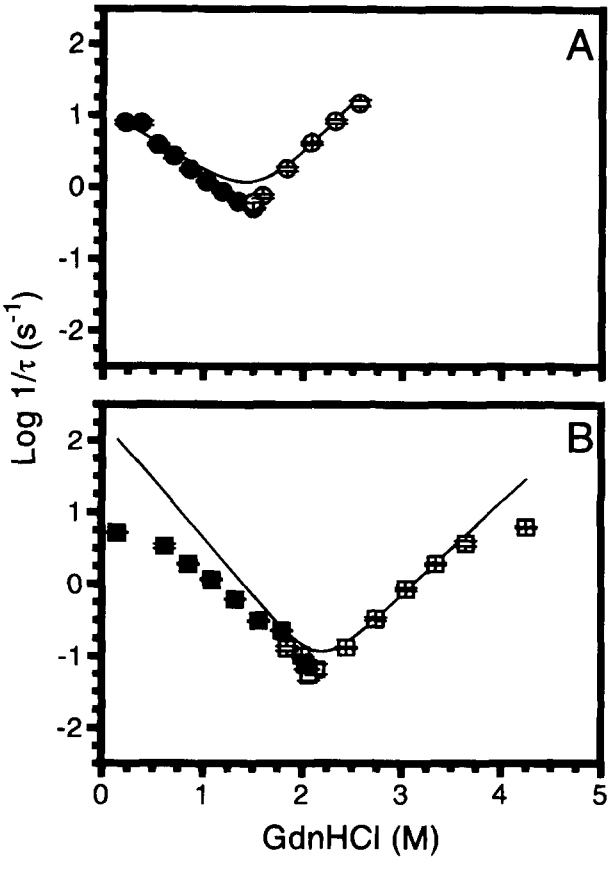

Fig. 8. Comparison of observed rates to calculated (two-state) rates for (**A**) iso-2 and (**B**) N52I iso-2. Predicted values of $\log(1/\tau)$ are calculated from a two-state analysis that combines equilibrium unfolding data (Fig. 3; Table 1) and unfolding kinetic data (Figs. 6, 7; Table 2) using methods described by Matouschek and co-workers (Matouschek et al., 1990). The solid line is the predicted (two-state) dependence of $\log(1/\tau)$ on the concentration of Gdn·HCl. The value of $1/\tau = k_{obs}$ is obtained from the sum of the observed unfolding rate constant (k_U) and a calculated value for the folding rate constant (k_F) obtained from the equation: $\log k_F = \log(k_U^\circ/K_U^\circ) - [(m - m_U^\ddagger)/(2.303RT)][\text{Gdn·HCl}]$. $K_U^\circ = \exp(-\Delta G_U^\circ/RT)$ is the unfolding equilibrium constant at 0.0 M Gdn·HCl.

The refolding rates (k_F) can be described by the similar equation:

$$\log k_F = \log k_F^\circ + [m_F^\ddagger/(2.303RT)][\text{Gdn·HCl}] \quad (2)$$

where k_F is the refolding rate constant, k_F° is the (extrapolated) refolding rate constant in the absence of denaturant, and $m_F^\ddagger$ is the denaturant dependence of the activation free energy for refolding ($m_F^\ddagger \equiv -d(\Delta G_F^\ddagger)/d[\text{Gdn·HCl}]$). The parameters describing the denaturant dependence of the refolding rate can be obtained directly by fitting the data to Equation 2. Alternatively, assuming that a two-state model gives an accurate description of both the equilibrium and kinetic properties of unfolding, k_F can be calculated from the observed least-squares fits of the unfolding rate data to Equation 1 and equilibrium unfolding data to the linear extrapolation model. This leads to the following relationship for calculating the refolding rate constant (Matouschek et al., 1990):

$$\log k_F = \log(k_U^\circ/K_U^\circ) + [(m_U^\ddagger - m)/(2.303RT)][\text{Gdn·HCl}] \quad (3)$$

were $K_U^\circ = \exp(-\Delta G_U^\circ/RT)$ and $m \equiv -d\Delta G_U/d[\text{Gdn·HCl}]$ are from the two-state analysis of the equilibrium unfolding experiments (Fig. 3; Table 1); and k_U° and $m_U^\ddagger$ are obtained from least-squares fits of the unfolding rate data to Equation 1. The solid lines in Figure 8, $\log(1/\tau) = \log(k_F + k_U)$, are obtained by calculating $\log(1/\tau)$ from the observed k_U (Equation 1) and the calculated k_F (Equation 3) as a test of whether folding is in accord with the predictions of a two-state kinetic mechanism. The kinetic parameters obtained from this analysis are summarized in Table 2. Figure 8 and Table 2 show that neither protein adheres strictly to the two-state model. For iso-2 the main discrepancy is in the observed and calculated values of $m_F^\ddagger$, but for N52I iso-2 there are large differences between the observed and calculated values of both $m_F^\ddagger$ and k_F°.

Kinetic amplitudes for iso-2 and N52I iso-2

The relative amplitude for fast phase (τ_2) folding is calculated as the fraction of the total kinetically detected folding associated with phase τ_2: $\alpha_2 = A_2/(A_2 + A_1)$, where A_i is the signal change associated with kinetic phase τ_i. For fluorescence-detected folding/unfolding, the dependence of the relative amplitude (α_2) on denaturant given in Figures 6A and 7A shows the same basic pattern, although the curve shifts to slightly higher Gdn·HCl concentration for N52I iso-2. For absorbance-detected folding/unfolding the relative amplitude (α_2) shows a different, more complex dependence on denaturant. The dependence of the amplitude on Gdn·HCl for iso-2 (Fig. S1A; supplementary materials) appears to shift to higher denaturant concentration for N52I iso-2 (Fig. S2A; supplementary materials), but for absorbance-detected folding there may also be differences in the functional dependence of the relative amplitudes on Gdn·HCl.

Kinetic amplitudes can also be measured relative to the total equilibrium signal change. Amplitudes measured in this way are referred to as absolute amplitudes. Absolute amplitudes are useful because they provide a test of whether all the phases in folding (or unfolding) are kinetically resolved within the stopped-flow time range (~2 ms–600 s). Very slow phases ($\tau > 600$ s) are easy to detect because very slow kinetic phases can be measured in manual mixing experiments using spectrophotometers or fluorimeters with much better time-dependent baseline stability than stopped-flow instruments. The presence of very slow kinetic phases can also be detected as hysteresis in equilibrium unfolding experiments when insufficient time is allotted to reach equilibrium. On the other hand, very fast kinetic phases ($\tau < 2$ ms) can be missed entirely by stopped-flow mixing experiments. The rates of kinetic phases that occur in times shorter than the mixing time (~2 ms) cannot be measured by stopped-flow mixing, but the amplitudes of these very fast "burst phases" can be estimated from the absolute amplitudes of the kinetically observed phases. The procedure is to sum the absolute amplitudes of all kinetically resolved phases and to assign any remaining signal changes to the "burst phase." Absolute amplitudes are also useful in estimating the fractional concentrations of species present in folding experiments.

The absolute amplitudes for fluorescence-detected folding of iso-2 and N52I iso-2 are given in Figure 9 for the kinetically unresolved "burst phase" and for the resolved fast (τ_2) and slow (τ_1) phases. The absolute amplitudes were determined by referencing fluorescence changes from equilibrium unfolding and from the slow kinetic phase (τ_1) in folding to a fluorescence standard, N-acetyltryptophanamide (NATA). In Figure 10A and B the sum

Table 2. *Kinetic parameters for iso-2 and N52I iso-2*[a]

Protein	k_U°[b] (s^{-1})	$m_U^{\ddagger}$[b] (kcal mol^{-1} M^{-1})	$k_{F_{obs}}^{\circ}$[c] (s^{-1})	$m_{F_{obs}}^{\ddagger}$[c] (kcal mol^{-1} M^{-1})	$k_{F_{calc}}^{\circ} = (k_U^{\circ}/K_U^{\circ})$[d] ($s^{-1}$)	$m_{F_{calc}}^{\ddagger} = (m_U^{\ddagger} - m)$[d] (kcal mol^{-1} M^{-1})
Iso-2 (WT)	$(4.2 \pm 0.1) \times 10^{-3}$	1.9 ± 0.1	14.4 ± 0.7	-1.40 ± 0.03	11.7 ± 0.1	-1.1 ± 0.2
N52I iso-2	$(9.3 \pm 0.8) \times 10^{-5}$	1.7 ± 0.1	17 ± 1	-1.47 ± 0.08	186 ± 19	-2.2 ± 0.2

[a]Errors are estimated from the statistics of nonlinear least-squares fits of the data (see Figs. 6, 7) using the program ENZFITTER (Leatherbarrow, 1987).

[b]k_U° and $m_U^{\ddagger}$ are obtained from the intercept and the slope of least-squares fits to the Gdn·HCl dependence of the unfolding rates (Figs. 6, 7) using the equation: $\log k_U = \log k_U^{\circ} + [m_U^{\ddagger}/(2.303RT)][\text{Gdn·HCl}]$.

[c]$k_{F_{obs}}^{\circ}$ and $m_{F_{obs}}^{\ddagger}$ are obtained from the intercept and the slope of least-squares fits to the Gdn·HCl dependence of the folding rates (Figs. 6, 7) using the equation: $\log k_{F,obs} = \log k_{F_{obs}}^{\circ} + [m_{F_{obs}}^{\ddagger}/(2.303RT)][\text{Gdn·HCl}]$.

[d]$k_{F_{calc}}^{\circ}$ and $m_{F_{calc}}^{\ddagger}$ are the calculated intercept and slope for refolding obtained from fits to the unfolding rates and the equilibrium data (Fig. 8). The least-squares fit is to the equation:

$$\log k_{F_{calc}} = \log(k_U^{\circ}/K_U^{\circ}) + [(m_U^{\ddagger} - m)/(2.303RT)][\text{Gdn·HCl}],$$

where

$$\log k_{F_{calc}}^{\circ} = \log(k_U^{\circ}/K_U^{\circ}) \quad \text{and} \quad m_{F_{calc}}^{\ddagger} = m_U^{\ddagger} - m.$$

of the absolute amplitudes for the fast (τ_2) and slow (τ_1) phases is plotted superimposed on the equilibrium transitions from Figure 3. In this representation the missing amplitude, or "burst phase," is the distance between the dashed line and the data points.

Discussion

Increases in the cooperativity of equilibrium unfolding for N52I iso-2

One of the most interesting results of the equilibrium unfolding experiments is the dramatic increase in the *m*-value of unfolding for the N52I substitution. The observed 30% increase in the *m*-value is much too large to be consistent with the usual interpretation of *m*-values as changes in exposure of solvent accessible hydrophobic surface (ΔASA) on unfolding (Myers et al., 1995). Correlations between ΔASA and the number of amino acid residues have been derived that indicate that iso-2 has the *m*-value expected for a globular protein of 112 residues. The anomalously large *m*-value of N52I iso-2 implies ΔASA = 17,700 Å^2 for unfolding, which is 86% larger than the expected ΔASA = 9,500 Å^2 for a protein of 112 residues (Myers et al., 1995). The N52I mutation-induced change, ΔΔASA, which is implied by the increase in *m*-value is much larger than is physically reasonable. The value of ΔΔASA = 8,200 Å^2 suggested by the *m*-value for N52I iso-2 is 240-fold greater than ΔΔASA = 34 Å^2 calculated for an Asn to Ile substitution assuming full burial of the standard state surface area of residue 52 (Rose et al., 1985).

The X-ray structure of N52I iso-2 is very similar to that of iso-2 except for the H-bonding changes near the heme shown in Figure 2A,B. Thus, while a comparison of the X-ray structures (Fig. 1) shows that Ile52 in N52I iso-2 buries more hydrophobic surface than Asn52 of iso-2, the changes (ΔΔASA) are much too small to explain the observed increase in *m*-value. The most significant differences observed from the X-ray structures are those detailed in Figure 2A and B. These differences include changes in the H-bond network near the heme, but also involve loss of conserved Wat106. Little is known about the consequences of the loss of a structural water molecule for protein stability or the cooperativity of unfold-

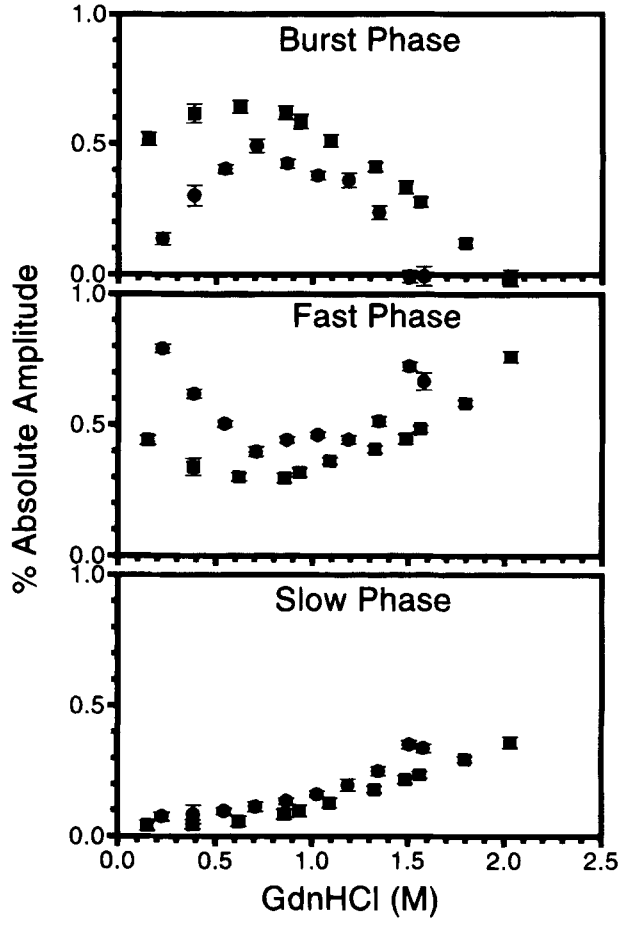

Fig. 9. Absolute amplitudes for fluorescence-detected folding. The Gdn·HCl dependence of the fluorescence-detected amplitudes is given as a fraction of the total equilibrium change for the "burst phase" (upper panel), fast phase (τ_2 phase; middle panel), and the slow phase (τ_1 phase; lower panel). Data for iso-2 are shown as filled circles and the data for N52I iso-2 are shown as filled squares. The absolute amplitudes are measured by referencing the fluorescence changes to NATA as described in Materials and methods.

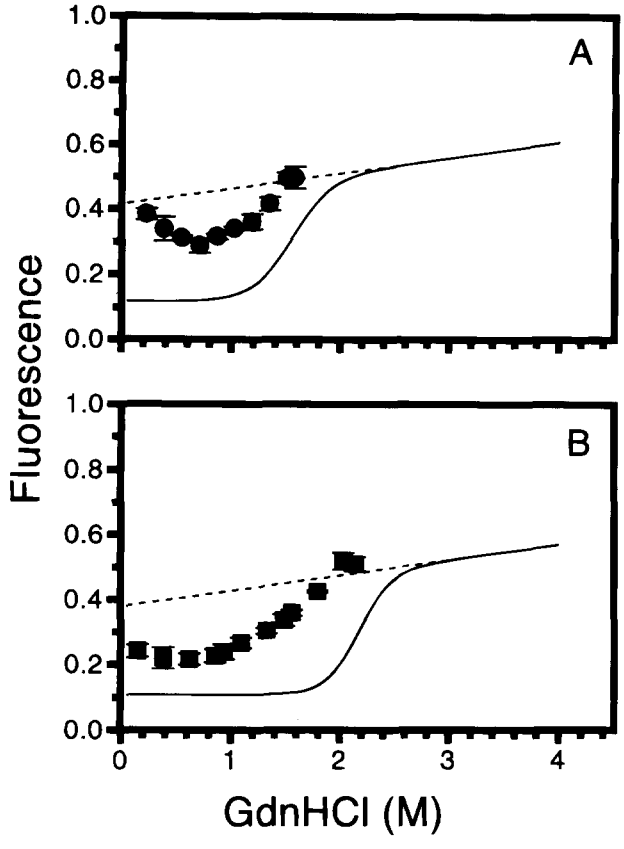

Fig. 10. Total kinetic amplitudes for refolding are shown for (**A**) iso-2 (filled circles) and (**B**) N52I iso-2 (filled squares). The total amplitudes are measured by referencing hand-mixing measurements of the amplitude for the fluorescence-detected slow-phase to the fluorescence of N-acetyltryptophanamide (NATA). Measurements of both the fast and the slow phase amplitudes by stopped-flow mixing allows calculation of the absolute amplitude for the fast phase from the (hand mixing) slow phase amplitude referenced to NATA. The total kinetic amplitude (sum of the fast and slow phase absolute amplitudes referenced to NATA) is plotted along with the equilibrium curve (solid line) from Figure 3. The dashed line gives the Gdn·HCl dependence of the fluorescence for the fully unfolded protein at equilibrium. The missing amplitude ("burst phase") is the distance between the dashed line and the data points.

ing. Assuming that mutation-induced changes in equilibrium unfolding are discernible as structural differences, then attention should be focused on Wat106 as a key residue in understanding the structural mechanism that results in such an unusually large increase in *m*-value.

Linear free-energy relationships and refolding rates

For all but the lowest Gdn·HCl concentrations the refolding branch for phase (τ_2) folding exhibits the expected linear dependence of $\log(1/\tau) \approx \log k_F$ on the concentration of Gdn·HCl. The equilibrium unfolding transition is well described by the linear extrapolation model, which assumes a linear dependence of the equilibrium unfolding free energy on the Gdn·HCl concentration. The fact that the activation free energy for folding ($\Delta G_F^{\ddagger}$) and the equilibrium free energy of unfolding (ΔG_U) are both linearly dependent on Gdn·HCl requires a linear free-energy relationship (Matouschek & Fersht, 1993) between the denaturant-induced changes in stability and folding rates. Such a relationship is expected for any protein that obeys both a two-state kinetic mechanism and the linear extrapolation model.

A more important question is whether a free-energy relationship exists for a series of related or "engineered" mutant proteins (Matouschek & Fersht, 1993). The existence of a free-energy relationship for related proteins can aid in understanding mechanistic aspects of folding, such as the degree of structural or thermodynamic similarity between the folding transition state and the native protein. The results with N52I iso-2 are unambiguous. N52I iso-2 is substantially more stable than iso-2 (Fig. 3, Table 1) but folds at the same rate (Figs. 4–7; Figs. S1–S2, supplementary materials), so there is no linear free-energy relationship between iso-2 and N52I iso-2. The fact that iso-2 and N52I iso-2 differ in stability but fold at the same rate suggests a common rate-limiting step not coupled to thermodynamic stability. The displacement of an incorrect His-heme ligand is thought to be rate limiting for folding of many cytochromes *c*, including both horse cytochrome *c* (Elove et al., 1994; Sosnick et al., 1994) and yeast iso-2 (Pierce & Nall, 1997). His-heme misligation will be unaffected by most mutations that alter thermodynamic stability, other than substitutions replacing His. Moreover, the off rate of His from an incorrect His-heme ligand complex is expected to be similar for many different cytochromes *c*, so folding rates will also be similar. In summary, the reason that iso-2 and N52I iso-2 have the same folding rates despite having different thermodynamic stabilities is that the rate of displacement of an incorrect His-heme ligand is rate limiting in folding of both proteins.

N52I and the transition states for folding and unfolding

The kinetic analogs of equilibrium *m*-values are useful in characterizing folding/unfolding transition states. Values of $m_U^{\ddagger}$ and $m_F^{\ddagger}$ listed in Table 2 can be interpreted in terms of ΔASA changes in a manner similar to that for the equilibrium *m*-value (Fersht, 1993; Matouschek & Fersht, 1993). The ratio of kinetic $m_i^{\ddagger}$-values to equilibrium *m*-values gives an estimate of the fractional change in ΔASA on forming the transition state for folding (or unfolding). For example in folding $(m_F^{\ddagger}/m) = -0.47 \pm 0.03$ for iso-2 and $(m_F^{\ddagger}/m) = -0.38 \pm 0.03$ for N52I iso-2, so on forming the transition state both proteins bury slightly less than half of the equilibrium change in hydrophobic surface. The negative signs show that the approach to the transition state for folding involves burial of hydrophobic surface (a negative fractional change in ΔASA), and the slightly more negative value for iso-2 indicates that transition from the starting state (either the unfolded protein, or a folding intermediate) to the transition state involves burial of more hydrophobic surface than for N52I iso-2. For unfolding, $(m_U^{\ddagger}/m) = 0.63 \pm 0.05$ for iso-2 and $(m_U^{\ddagger}/m) = 0.44 \pm 0.03$ for N52I iso-2, suggesting that iso-2 exposes slightly more hydrophobic surface than N52I iso-2 to reach the unfolding transition state.

It is important to keep in mind that the relationship between *m*-values and hydrophobic surface exposure is very uncertain, especially for N52I iso-2, which has an anomalously high equilibrium *m*-value. Deviations from a two-state kinetic mechanism (which will be discussed below) make the supposed relationship between the kinetic *m*-values and changes in hydrophobic surface even more tenuous. In the presence of folding intermediates, it is not always clear whether the same initial states are involved for folding or unfolding, or whether the transition states are similar. It is interesting to compare our *m*-values to those obtained by others

with the closely related protein, yeast iso-1 cytochrome *c*. For iso-1 the N52I mutation-induced change in the equilibrium *m*-value is similar in magnitude but opposite in sign to that observed for iso-2. There are also differences in our kinetic *m*-values and those reported for iso-1 (Doyle et al., 1996). Clearly, our understanding of both kinetic and equilibrium *m*-values leaves much to be desired.

The m-value test for folding intermediates

An important test for folding intermediates has been devised by comparing equilibrium and kinetic *m*-values for consistency with two-state folding/unfolding (Matouschek et al., 1989; Matouschek & Fersht, 1993; Parker et al., 1995). The test is based on the assumption that unfolding is more likely to be kinetically two-state than refolding, because unfolding conditions (high temperatures, extremes of pH, or high concentrations of denaturants) destabilize most folding intermediates. The results of this test are summarized in Table 2 and in Figure 8. The deviations from two-state behavior for iso-2 are modest, but those for N52I iso-2 are substantial for both $m_F^{\ddagger}$ and k_F°. This suggests that the N52I substitution induces the formation of a transient folding intermediate, or enhances the stability of an intermediate already present in folding of iso-2. Results presented in the next section suggest that it is the latter that is most likely.

Absolute amplitudes and folding intermediates

With certain mechanistic assumptions, the absolute amplitudes plotted in Figure 9 can give estimates of the Gdn·HCl dependence of the population of various species in folding. The following highly simplified scheme (Equation 4) helps in understanding the absolute amplitude behavior for folding of iso-2 and N52I iso-2:

$$\begin{array}{ccccccc} & U_S & \text{slow} & U_F & & & \\ \text{very fast} & \uparrow\downarrow & \rightarrow & \uparrow\downarrow & \text{very fast} & \underset{\rightarrow}{\text{fast}} & \\ & I_S & \text{slow} & I_F & & & N \end{array} \qquad (4)$$

The U_S and U_F species are fully unfolded species differing only in the isomerization state of one or more of the five prolines in iso-2 and N52I iso-2. The U_S species have at least one non-native *cis* proline, so folding of these species will be very slow because it requires proline isomerization. The U_F species are assumed to have all prolines in the *trans* (native) isomeric state, so the U_F species fold without the need to isomerize a proline. The I_i species are kinetically trapped "native-like" folding intermediates with an incorrect proline isomer (I_S) or a misligated heme (I_F). The I_i species are compact species assumed to have optical properties (fluorescence) similar to that of the native protein, the *N* species. Conversion of the I_S species to the I_F species is slow because the reaction involves an intrinsically slow process, proline isomerization. The I_F to *N* process is fast but is limited in rate by displacement of an incorrect His-heme ligand. The U_S to I_S and U_F to I_F reactions are both very fast structure-forming reactions that take place in the stopped-flow mixing dead time. The kinetically trapped I_i species maintain a very fast pre-equilibrium with the U_i species. The U_i species are fully unfolded while the I_i species have "native-like" fluorescence properties, so most if not all of the fluorescence changes take place in the U_i to I_i reaction. The main features of scheme 4 are taken from a mechanism developed previously to describe coupling of structure-formation to proline isomerization (Osterhout & Nall, 1985; Nall, 1996), and are similar to a more detailed mechanism (Colon et al., 1996) used to describe the kinetics of folding of mutational variants of horse cytochrome *c*.

Using scheme 4, the "burst phase" amplitude is a measure of the pre-equilibrium distribution of species between unfolded U_i species and collapsed I_i species (optically "native-like"). For both iso-2 and N52I iso-2 the "burst phase" amplitude increases from zero to 0.7 M Gdn·HCl, suggesting that low concentrations of Gdn·HCl stabilize these species. The Gdn·HCl stabilizing effect may be similar to that observed for horse cytochrome *c* at low pH (Tsong, 1975) where the stabilizing effects have been attributed to a chloride ion salt effect. Above 0.7 M Gdn·HCl the "burst phase" amplitude drops, suggesting that the I_i species are destabilized by high concentrations of Gdn·HCl as the denaturing effects of Gdn·HCl overwhelm the stabilizing salt effects. The behavior of the fast phase (τ_2) absolute amplitude is the mirror image of the "burst phase." This is because more of the fluorescence change occurs within the mixing deadtime ("burst phase") when the pre-equilibrium favors the I_F species, but the fluorescence changes are rate limited by the I_F to *N* reaction when the pre-equilibrium favors the U_F species. Surprisingly, the absolute amplitude behavior of the slow phase (τ_1) shows little evidence of a stabilizing salt effect at low Gdn·HCl concentrations. This may be because of differences in the kinetic blocks: a misligated His-heme complex may be more destabilizing to the I_F species than a *cis* proline is for the I_S species. Nevertheless, the absolute amplitude of the slow phase (τ_1) rises slowly as the Gdn·HCl concentration increases suggesting a gradual shift in the U_S to I_S pre-equilibrium toward the U_S species. Alternatives to scheme 4 include mechanisms in which the I_F species are off pathway and must be unfolded (to U) before refolding to *N*. Distinctions between on- and off-pathway mechanisms are subtle, and require additional assumptions not tested by kinetic data (Khorasanizadeh et al., 1996).

A comparison of the absolute amplitude behavior of iso-2 with N52I iso-2 leads to the conclusion that the N52I substitution is stabilizing for all structured species: I_S, I_F, and *N*. The N52I substitution increases the absolute amplitude for the "burst phase" implying shifts in the U_S to I_S pre-equilibrium toward I_S and the U_F to I_F pre-equilibrium toward I_F. As expected, the N52I substitution leads to corresponding drops in the absolute amplitudes for the fast phase (τ_2), and for the slow phase (τ_1). The pattern of stability enhancement for the I_S and I_F species by the N52I substitution is even more apparent in Figure 10, which plots the sum of the fast and slow phase absolute amplitudes versus Gdn·HCl. For kinetic refolding experiments ending in the native baseline region, the fluorescence immediately following mixing is closer to that of the native species for N52I iso-2 than for iso-2.

Conclusions

The N52I substitution results in a higher midpoint (C_m) for guanidine hydrochloride (Gdn·HCl) unfolding and a larger unfolding free energy, ΔG_U°. For standard conditions (pH 6, 0.1 M sodium phosphate, 20 °C) $C_m = 2.2 \pm 0.2$ M, $\Delta G_U^{\circ} = 8.5 \pm 0.5$ kcal mol^{-1} for N52I iso-2; and $C_m = 1.5 \pm 0.2$ M, $\Delta G_U^{\circ} = 4.6 \pm 0.3$ kcal mol^{-1} for iso-2. The N52I substitution also increases the equilibrium *m*-value ($m \equiv -d\Delta G_U/d[\text{Gdn·HCl}]$). The *m*-value has been correlated with changes in solvent accessible hydrophobic surface on unfolding (Myers et al., 1995), so the change in *m*-value from $m = 3.0 \pm 0.2$ kcal mol^{-1} M^{-1} (iso-2) to $m = 3.9 \pm 0.2$ kcal mol^{-1} M^{-1} (N52I iso-2) suggests that the N52I substitution in-

creases the exposure of hydrophobic surface on unfolding. However, the mutation-induced changes in the exposure of hydrophobic surface area on unfolding that are estimated from the X-ray structures of iso-2 and N52I iso-2 are two orders of magnitude too small to explain the anomalously large change in m-value. The major mutation-induced change in structure, loss of conserved Wat106, may play a role in increasing the unfolding m-value by an mechanism unrelated to changes in solvent accessible surface.

Kinetic $m_i^{\ddagger}$ ($m_i^{\ddagger} \equiv -d\Delta G_i^{\ddagger}/d[\text{Gdn·HCl}]$) are obtained from the denaturant dependence of the activation free energy for fast phase folding ($m_i^{\ddagger}$) and unfolding ($m_u^{\ddagger}$). For refolding the measured values for $m_i^{\ddagger}$ are similar for iso-2 ($m_f^{\ddagger} = -1.40 \pm 0.03$ kcal mol^{-1} M^{-1}) and N52I iso-2 ($m_f^{\ddagger} = -1.47 \pm 0.08$ kcal mol^{-1} M^{-1}). For unfolding $m_u^{\ddagger} = 1.91 \pm 0.07$ kcal mol^{-1} M^{-1} for iso-2 and decreases to $m_u^{\ddagger} = 1.73 \pm 0.05$ kcal mol^{-1} M^{-1} for N52I iso-2. The change in $m_u^{\ddagger}$ suggests that the N52I substitution decreases the change in solvent accessible hydrophobic surface between the native state and the unfolding transition state.

For N52I iso-2, there are no changes in refolding rate for the fast phase (τ_2) or the proline isomerization-limited slow phase (τ_1), but the fast phase (τ_2) unfolding rate decreases. For iso-2 and especially for N52I iso-2, the observed fast phase (τ_2) refolding rate constants deviate from those calculated with a two-state model that combines (unfolding) kinetic and equilibrium data. Folding intermediates are detected for both proteins as kinetically unresolved signal changes ("burst phase") within the stopped-flow dead time ($\tau_d < 4$ ms). The "burst phase" amplitude is larger for N52I iso-2, suggesting that the N52I substitution stabilizes the "burst phase" intermediates. Free energy diagrams in Figure 11 account for the N52I mutation-induced effects on the kinetics of folding/unfolding and on the "burst phase" amplitude. The diagrams (Fig. 11A,B) make use of the thermodynamic parameters of Table 1 and the kinetic parameters of Table 2, and are constructed to correspond to the refolding conditions of Figure 4 (0.6 M Gdn·HCl, pH 6, 20 °C), and the unfolding conditions of Figure 5 (2.8 M Gdn·HCl, pH 6, 20 °C). The unfolded state, U, is taken as the reference state in which the free energies of the normal and mutant proteins are assumed to be the same. For refolding (Fig. 11A) the N52I substitution stabilizes the I-state and T-state (the transition state) by the same amount, so there is no change in the activation free energy barrier to refolding. For unfolding (Fig. 11B) the N52I substitution slows unfolding by (1) stabilizing the N-state, and (2) destabilizing the T-state. Note that the mutational effects on the transition state, T, have opposite signs for unfolding and refolding: the N52I substitution stabilizes the T-state for refolding, but destabilizes the T-state for unfolding.

In summary, the effects of the "global suppressor" N52I substitution are to: (1) increase the equilibrium thermodynamic stability; (2) enhance the stability of transiently populated "burst phase" folding intermediates; and (3) decrease the fast phase (τ_2) unfolding rate.

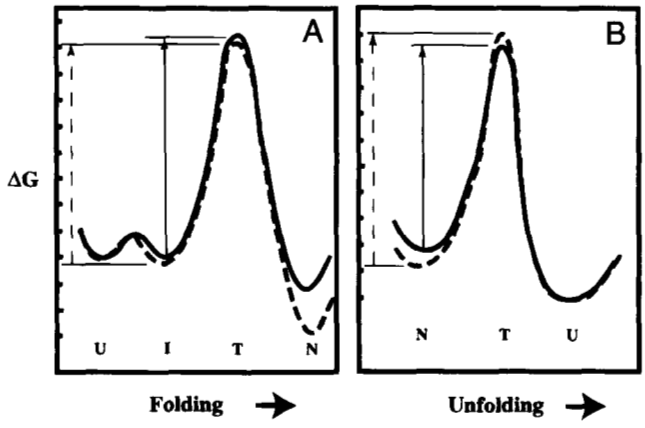

Fig. 11. Free-energy diagrams for (**A**) refolding and (**B**) unfolding of iso-2 (solid line) and N52I iso-2 (dashed line). All free energies are given as differences relative to a (reference) unfolded state (U); i.e., $\Delta G \approx 0$ for the U-state of both proteins. Note that equilibrium m-value differences (Table 1) and N52I hydrophobicity changes suggest that unfolded iso-2 and unfolded N52I iso-2 will differ on an absolute free-energy scale. The equilibrium free-energy differences are calculated using the thermodynamic parameters given in Table 1. Refolding (**A**) corresponds to the conditions of Figure 4: 0.6 M Gdn·HCl, pH 6, 20 °C. Unfolding (**B**) corresponds to the conditions of Figure 5: 2.8 M Gdn·HCl, pH 6, 20 °C. For both refolding and unfolding each division on the ΔG axis corresponds to about 2 kcal mol^{-1}. The N52I substitution stabilizes the T-state (transition state) for refolding slightly (**A**), but destabilizes the T-state for unfolding (**B**). Presumably, the differences in the mutational effects on the transition states for refolding and unfolding arise from the different denaturant concentrations used for the two experiments: 0.6 M Gdn·HCl for refolding, vs. 2.8 M Gdn·HCl for unfolding. In (**B**) the I-state is not shown because it is assumed that intermediates are melted out by the high denaturant concentrations used for the unfolding experiments. No attempt has been made to relate m-values to the reaction coordinates because of the uncertainty in interpretation of the kinetic and equilibrium m-values (see text).

Materials and methods

The construction, purification, and characterization of iso-2 and N52I iso-2 have been previously described (Nall & Landers, 1981; McGee et al., 1996).

Equilibrium unfolding

An 8 M stock of guanidine hydrochloride (ICN Biomedical Inc., Aurora, Ohio) was prepared in 0.1 M sodium phosphate, pH 6.0. The Gdn·HCl concentration was determined from measurements of refractive index (Pace, 1986). The 8-M stock was used to prepare all subsequent guanidine hydrochloride solutions. Protein samples were prepared by dissolving 20 mg of lyophilized protein in 2.0 mL of 4.5 M Gdn·HCl, 0.1 M sodium phosphate, pH 6.0. The protein solution was heated to 60 °C for 10 min to disrupt possible aggregated protein formed during the lyophilization process.

Fluorescence measurements were made on a SLM Aminco SPF-500C spectrofluorimeter (SLM Instruments, Inc., Urbana, IL) at 350 nm with excitation at 285 nm. Guanidine hydrochloride solutions of various concentrations were prepared with a final protein concentration of 4 μM for both iso-2 and N52I iso-2. Fluorescence measurements were made relative to an equal molar concentration of N-acetyltryptophanamide (NATA). The temperature was maintained at 20 °C throughout the experiments. The data were analyzed using the method described by Santoro and Bolen (Santoro & Bolen, 1988) using the non-linear least-squares program ENZFITTER (Leatherbarrow, 1987).

Kinetic experiments

Stopped-flow experiments were carried out using a three syringe Biologic SFM-3 stopped-flow (Molecular Kinetics, Inc., Pullman, WA). Fluorescence was measured at a right angle to incident 285 nm light through a 360 nm (300–400 nm) bandpass filter. The initial conditions for iso-2 were 200 μM iso-2 and 4.5 M Gdn·HCl

for refolding experiments or 0.4 M Gdn·HCl for unfolding experiments. A mixing ratio of 1:19 (for refolding and unfolding) gave final iso-2 concentrations for fluorescence-detected stopped-flow experiments of 10 μM. The same conditions were used for fluorescence-detected stopped flow measurements of N52I iso-2 except that initial N52I iso-2 concentrations were 275 μM for refolding and 166 μM for unfolding. Mixing ratios of 1:29 for refolding and 1:14 for unfolding gave final N52I iso-2 concentrations of 9 μM (refolding) and 10 μM (unfolding). Stopped-flow absorbance measurements were carried out at 418 nm. For iso-2 the experimental conditions were the same as for the fluorescence-detected stopped-flow experiments except that the initial protein concentration (unfolding and refolding) was 450 μM, with a 1:9 dilution ratio to give final protein concentrations (unfolding and refolding) of 45 μM. Absorbance-detected stopped-flow measurements of N52I iso-2 were carried out in the same way as for iso-2 except that the initial and final N52I iso-2 concentrations were 400 and 40 μM, respectively. All stopped-flow experiments were carried out at 20 °C in the presence of 0.1 M sodium phosphate, pH 6.0. To collect the fast and slow phases simultaneously, the optical signal was split and collected on two different time scales. Data were collected and analyzed with the Bio-Kine software supplied by Biologic. The relative amplitude, α, was calculated as follows: $\alpha = A_2/(A_2 + A_1)$, where A_2 and A_1 are the fast phase and slow phase amplitudes, respectively.

The slow phase refolding (τ_1) was measured by manual mixing in addition to stopped-flow mixing. Fluorescence hand-mixing experiments for iso-2 and N52I iso-2 were carried out on an SLM/Aminco SPF-500C spectrofluorimeter. Fluorescence-detected hand mixing experiments used initial protein concentrations of 800 μM and mixing ratios of 1:199 to give final protein concentrations of 4 μM (0.1 M sodium phosphate, pH 6.0, 20 °C). The emission wavelength was 350 nm with an excitation wavelength of 285 nm. Fluorescence intensity was measured relative to the signal intensity of an equal molar concentration of N-acetyltryptophanamide (NATA) to provide an absolute measure of slow phase fluorescence signal changes. Absorbance hand-mixing experiments were carried out on a Hewlett-Packard HP8452A diode array spectrophotometer at 418, 394, and 280 nm. Initial and final conditions for absorbance-detected hand mixing experiments were similar to those used for fluorescence, except that the final protein concentrations were 15–20 μM. All kinetic data were analyzed using the Bio-Kine software.

Acknowledgments

The authors thank Dr. Susan Weintraub for help with the electrospray ion mass spectrometry, Sofia Ghidarpour for construction of the N52I iso-2 containing yeast strain, and Michael M. Pierce for comments on the manuscript. Figures 1 and 2 were prepared using MidasPlus from the Computer Graphics Laboratory, University of California, San Francisco (Ferrin et al., 1988). This work was supported by grants from the National Institute of General Medical Sciences (GM32980), the National Center for Research Resources (RR05043), and the Robert A. Welch Foundation (AQ838).

References

Berghuis AM, Guillemette JG, McLendon G, Sherman F, Smith M, Brayer GD. 1994. The role of a conserved internal water molecule and its associated hydrogen bond network in cytochrome *c*. *J Mol Biol 236*:786–799.

Berroteran RW, Hampsey M. 1991. Genetic analysis of yeast iso-1-cytochrome *c* structural requirements: Suppression of Gly6 replacements by an Asn52–Ile replacement. *Arch Biochem Biophys 288*:261–269.

Colon W, Elove GA, Wakem LP, Sherman F, Roder H. 1996. Side chain packing of the N- and C-terminal helices plays a critical role in the kinetics of cytochrome *c* folding. *Biochemistry 35*:5538–5549.

Das G, Hickey DR, McLendon D, McLendon G, Sherman F. 1989. Dramatic thermostabilization of yeast iso-1-cytochrome *c* by an asparagine–isoleucine replacement at position 57. *Proc Natl Acad Sci USA 86*:496–499.

Doyle DF, Waldner JC, Parikh S, Alcazar-Roman L, Pielak GJ. 1996. Changing the transition state for protein (un) folding. *Biochemistry 35*:7403–7411.

Elove GA, Bhuyan AK, Roder H. 1994. Kinetic mechanism of cytochrome *c* folding: Involvement of the heme and its ligands. *Biochemistry 33*:6925–6935.

Elove GA, Chaffotte AF, Roder H, Goldberg ME. 1992. Early steps in cytochrome *c* folding probed by time-resolved circular dichroism and fluorescence spectroscopy. *Biochemistry 31*:6876–6883.

Ferrin TE, Huang CC, Jarvis LE, Langridge R. 1988. The MIDAS display system. *J Mol Graphics 6*:13–27, 36–37.

Fersht AR. 1993. The sixth Datta lecture. Protein folding and stability: The pathway of folding of barnase. *FEBS Lett 325*:5–16.

Gao Y, McLendon G, Pielak GJ, Williams RJ. 1992. Electron-proton coupling in cytochrome *c* studied using protein variants. *Eur J Biochem 204*:337–352.

Hickey DR, Berghuis AM, Lafond G, Jaeger JA, Cardillo TS, McLendon D, Das G, Sherman F, Brayer GD, McLendon G. 1991. Enhanced thermodynamic stabilities of yeast iso-1-cytochromes *c* with amino acid replacements at positions 52 and 102. *J Biol Chem 266*:11686–11694.

Ikai A, Fish WW, Tanford C. 1973. Kinetics of unfolding and refolding of proteins. II. Results for cytochrome *c*. *J Mol Biol 73*:165–184.

Khorasanizadeh S, Peters ID, Roder H. 1996. Evidence for a three-state model of protein folding from kinetic analysis of ubiquitin variants with altered core residues. *Nat Struct Biol 3*:193–205.

Knapp JA, Pace CN. 1974. Guanidine hydrochloride and acid denaturation of horse, cow, and Candida krusei cytochromes *c*. *Biochemistry 13*:1289–1294.

Komar-Panicucci S, Weis D, Bakker G, Qiao T, Sherman F, McLendon G. 1994. Thermodynamics of the equilibrium unfolding of oxidized and reduced *Saccharomyces cerevisiae* iso-1-cytochromes *c*. *Biochemistry 33*:10556–10560.

Leatherbarrow RJ. 1987. *Enzfitter, a non-linear regression data analysis program for the IBM PC*. Cambridge: Biosoft.

Louie GV, Brayer GD. 1990. High-resolution refinement of yeast iso-1-cytochrome *c* and comparisons with other eukaryotic cytochromes *c*. *J Mol Biol 214*:527–555.

Matouschek A, Fersht AR. 1993. Application of physical organic chemistry to engineered mutants of proteins: Hammond postulate behavior in the transition state of protein folding. *Proc Natl Acad Sci USA 90*:7814–7818.

Matouschek A, Kellis JJ, Serrano L, Bycroft M, Fersht AR. 1990. Transient folding intermediates characterized by protein engineering. *Nature 346*:440–445.

Matouschek A, Kellis JJ, Serrano L, Fersht AR. 1989. Mapping the transition state and pathway of protein folding by protein engineering. *Nature 340*:122–126.

Matthews JM, Fersht AR. 1995. Exploring the energy surface of protein folding by structure–reactivity relationships and engineered proteins: Observation of Hammond behavior for the gross structure of the transition state and anti-Hammond behavior for structural elements for unfolding/folding of barnase. *Biochemistry 34*:6805–6814.

McGee WA, Rosell FI, Liggins JR, Rodriguez-Ghidarpour S, Luo Y, Chen J, Brayer GD, Mauk AG, Nall BT. 1996. Thermodynamic cycles as probes of structure in unfolded proteins. *Biochemistry 35*:1995–2007.

Mines GA, Pascher T, Lee SC, Winkler JR, Gray HB. 1996. Cytochrome *c* folding triggered by electron transfer. *Chem Biol 3*:491–497.

Murphy ME, Nall BT, Brayer GD. 1992. Structure determination and analysis of yeast iso-2-cytochrome *c* and a composite mutant protein. *J Mol Biol 227*:160–176.

Murphy MEP. 1993. Structural constraints for the folding, stability, and function of cytochrome *c* [PhD Thesis]. University of British Columbia.

Myers JK, Pace CN, Scholtz JM. 1995. Denaturant m values and heat capacity changes: Relation to changes in accessible surface areas of protein unfolding. *Protein Sci 4*:2138–2148.

Nall BT. 1983. Structural intermediates in folding of yeast iso-2 cytochrome *c*. *Biochemistry 22*:1423–1429.

Nall BT. 1996. Cytochrome *c* folding and stability. In: Scott RA, Mauk AG, eds. *Cytochrome c. A multidisciplinary approach*. Sausalito: University Science Books. pp 167–200.

Nall BT, Landers TA. 1981. Guanidine hydrochloride induced unfolding of yeast iso-2 cytochrome *c*. *Biochemistry 20*:5403–5411.

Nall BT, Osterhout JJ, Ramdas L. 1988. pH dependence of folding of iso-2-cytochrome *c*. *Biochemistry 27*:7310–7314.

Osterhout JJ, Nall BT. 1985. Slow refolding kinetics in yeast iso-2 cytochrome *c*. *Biochemistry 24*:7999–8005.

Pace CN. 1986. Determination and analysis of urea and guanidine hydrochloride denaturation curves. *Methods Enzymol 131*:266–280.

Parker MJ, Spencer J, Clarke AR. 1995. An integrated kinetic analysis of intermediates and transition states in protein folding reactions. *J Mol Biol 253*:771–786.

Pierce MM, Nall BT. 1997. Fast folding of cytochrome *c*. *Protein Sci 6*:618–627.

Rose GD, Geselowitz AR, Lesser GJ, Lee RH, Zehfus MH. 1985. Hydrophobicity of amino acid residues in globular proteins. *Science 229*:834–838.

Santoro MM, Bolen DW. 1988. Unfolding free energy changes determined by the linear extrapolation method. 1. Unfolding of phenylmethanesulfonyl alpha-chymotrypsin using different denaturants. *Biochemistry 27*:8063–8068.

Schindler T, Herrler M, Marahiel MA, Schmid FX. 1995. Extremely rapid protein folding in the absence of intermediates. *Nat Struct Biol 2*:663–673.

Shortle D, Lin B. 1985. Genetic analysis of staphylococcal nuclease: Identification of three intragenic global suppressors of nuclease-minus mutants. *Genetics 110*:539–555.

Sosnick TR, Mayne L, Hiller R, Englander SW. 1994. The barriers in protein folding. *Nat Struct Biol 1*:149–156.

Sosnick TR, Shtilerman MD, Mayne L, Englander SW. 1997. Ultrafast signals in protein folding and the polypeptide contracted state. *Proc Natl Acad Sci USA 94*:8545–8550.

Tsong TY. 1975. An acid induced conformational transition of denatured cytochrome *c* in urea and guanidine hydrochloride solutions. *Biochemistry 14*:1542–1547.

Tsong TY. 1976. Ferricytochrome *c* chain folding measured by the energy transfer of tryptophan 59 to the heme group. *Biochemistry 15*:5467–5473.

Veeraraghavan S, Rodriguez-Ghidarpour S, MacKinnon C, McGee WA, Pierce MM, Nall BT. 1995. Prolyl isomerase as a probe of stability of slow-folding intermediates. *Biochemistry 34*:12892–12902.